CROP: Contextual Region-Oriented Visual Token Pruning

Jiawei Guo^{1,2}, Feifei Zhai^{⊠1,3}, Pu Jian^{1,2}, Qianrun Wei^{1,2}, Yu Zhou^{1,3}

¹ State Key Laboratory of Multimodal Artificial Intelligence Systems,

Institute of Automation, CAS, Beijing, China

² School of Artificial Intelligence, University of Chinese Academy of Sciences, Beijing, China ³ Fanyu AI Laboratory, Zhongke Fanyu Technology Co., Ltd, Beijing, China {feifei.zhai, yzhou}@ia.ac.cn

Abstract

Current VLM-based VQA methods often process entire images, leading to excessive visual tokens that include redundant information irrelevant to the posed question. This abundance of unnecessary image details creates numerous visual tokens, drastically increasing memory and computational requirements in VLMs. To address this, we propose Contextual Region-Oriented Visual Token Pruning (CROP), a novel framework to compress visual tokens through a two-step process: Localization and Pruning. Specifically, CROP first employs an efficient model to identify the contextual region relevant to the input query. Subsequently, two distinct strategies are introduced for pruning: (1) Pre-LLM Compression (PLC), which adaptively compresses different image regions with varying ratios, and (2) Inner-LLM Pruning (ILP), a training-free method that prunes tokens within early LLM layers guided by the identified contextual region. Extensive experiments on a wide range of VQA tasks demonstrate that CROP significantly outperforms existing visual token pruning methods and achieves state-of-the-art performance. Our code and datasets will be made available.

1 Introduction

Recently, visual question answering (VQA) have achieved remarkable progress due to the rapid development of vision language Models (VLMs) (Bai et al., 2023; Yin et al., 2023; Li et al., 2024b; Ren et al., 2024; Singh et al., 2019; Zhou et al., 2025). Current VLM-based VQA methods utilize information from the entire image, but for specific questions, we need to locate local image regions to support the answer. Moreover, redundant image information also introduce a large number of visual tokens, requiring much higher memory and computation in VLMs (Zhang et al., 2025b; Huang et al., 2024). For example, there are 576 visual tokens in

LLaVA-1.5 (Liu et al., 2023), and the number is 2880 for a 672*672 image in LLaVA-NeXT (Yang et al., 2024).

For example in Figure 1(a), we actually only need a small region to answer the question, but still have to transform the entire image into so many visual tokens. To overcome this problem, visual token pruning methods have been emerged. Some methods reduce visual tokens before inputting them into LLM (Huang et al., 2024), which primarily depend on intrinsic image semantics. Others perform pruning inside the early LLM layers, usually on the basis of attention map (Chen et al., 2024). However, these methods fail to account for the input question, which might ignore the key task-relevant information (Li et al., 2024a).

In this paper, we introduce a novel framework Contextual Region-Oriented Vision Token Pruning (CROP) to facilitate effective visual tokens pruning. Here, contextual region is defined as a visual and coherence region of input image, which captures the key information for answering the question. The proposed CROP framework comprise two steps of Localization and Pruning. During Localization Stage, we develop an efficient model to identify the contextual region (L-CR). After that, in Pruning Stage, we take the region as a key information source and propose two simple but effective ways for pruning: Pre-LLM Compression (PLC) and Inner-LLM Pruning (ILP).

In PLC method, we propose a compression module that adaptively adjusts the compression ratio, assigning a lower compression ratio to the contextual region obtained from the localization stage, and a higher ratio otherwise. The ILP method prunes visual tokens in the LLM layers by the guidance of L-CR. Extensive experiments on a wide range of VQA benchmarks show that the proposed PLC and ILP methods consistently outperform the existing compression techniques, and achieve the state-of-the-art performance.



Figure 1: Comparison of different visual token pruning. (a) The input image and question. The red rectangle shows the region containing the answer of the question. (b) The visualization of retained tokens by attention-based pruning method. (c) The visualization of identified contextual region by our CROP framework.

The main contributions of this paper are summarized as follows:

- We develop an efficient Localization model to identify contextual regions, which serve as a plug-and-play component for guiding visual token pruning.
- We introduce a novel contextual regionoriented vision token pruning framework, and develop two different approaches on pruning, PLC and ILP. To our best knowledge, this is the first work of introducing contextual regions for visual tokens pruning.
- Experimental results demonstrate that our proposed method achieves state-of-the-art performance without requiring any training or fine-tuning in ILP method.

2 Related Works

2.1 Vision Token Reduction in VLMs

In VLMs, the number of input visual tokens often vastly exceeds that of text tokens, sometimes by orders of magnitude (Yao et al., 2024). Consequently, visual token pruning and compression have become significant research areas, with numerous studies emerging in recent years. Architecturally, these methods primarily differ by where pruning or compression occurs: some operate within the visual encoder, others function between the visual encoder and the LLM backbone (often termed Pre-LLM compression), and some perform pruning within the LLM backbone itself (commonly known as Inner-LLM pruning) (Han et al., 2025; Ye et al., 2025; Yan et al., 2024).

For instance, methods like Vision Zip (Yang et al., 2024) aim to retain high-attention visual tokens from the visual encoder while compressing or merging the rest. Focusing on Inner-LLM strategies, FastV (Chen et al., 2024) leverages crossmodal attention from intermediate model layers to select a Top-R set of visual tokens, pruning the remainder. To enhance the precision of crossmodal attention for token selection, TwigVLM (Shao et al., 2025) incorporates additional trainable layers within the model specifically for this purpose. SparseVLM (Zhang et al., 2024) notes the sparsity in text tokens as well and employs bidirectional selection of both text and visual tokens to extract more informative visual representations. Addressing Pre-LLM compression, LLaVA-Mini (Zhang et al., 2025b) introduces an external prefusion module that performs cross-modal information fusion before the LLM, enabling visual token merging.

However, a common characteristic of these compression techniques is their tendency to yield fragmented and discrete visual tokens. This can disrupt the original spatial semantics and continuity of visual regions. Such an approach may inadvertently retain trivial, peripheral, or low-information visual tokens, potentially hindering the VLM's visual perception capabilities (Shao et al., 2024). In contrast, our CROP method focuses on identifying contiguous spatial regions directly relevant to the input question. By doing so, CROP aims to preserve more of the main visual object's information and provide more semantically valuable visual context to the LLM.

2.2 Key Region Perception in VLMs

Recent advancements have demonstrated that VLMs possess a notable capability to identify and ground information within specific visual spatial re-

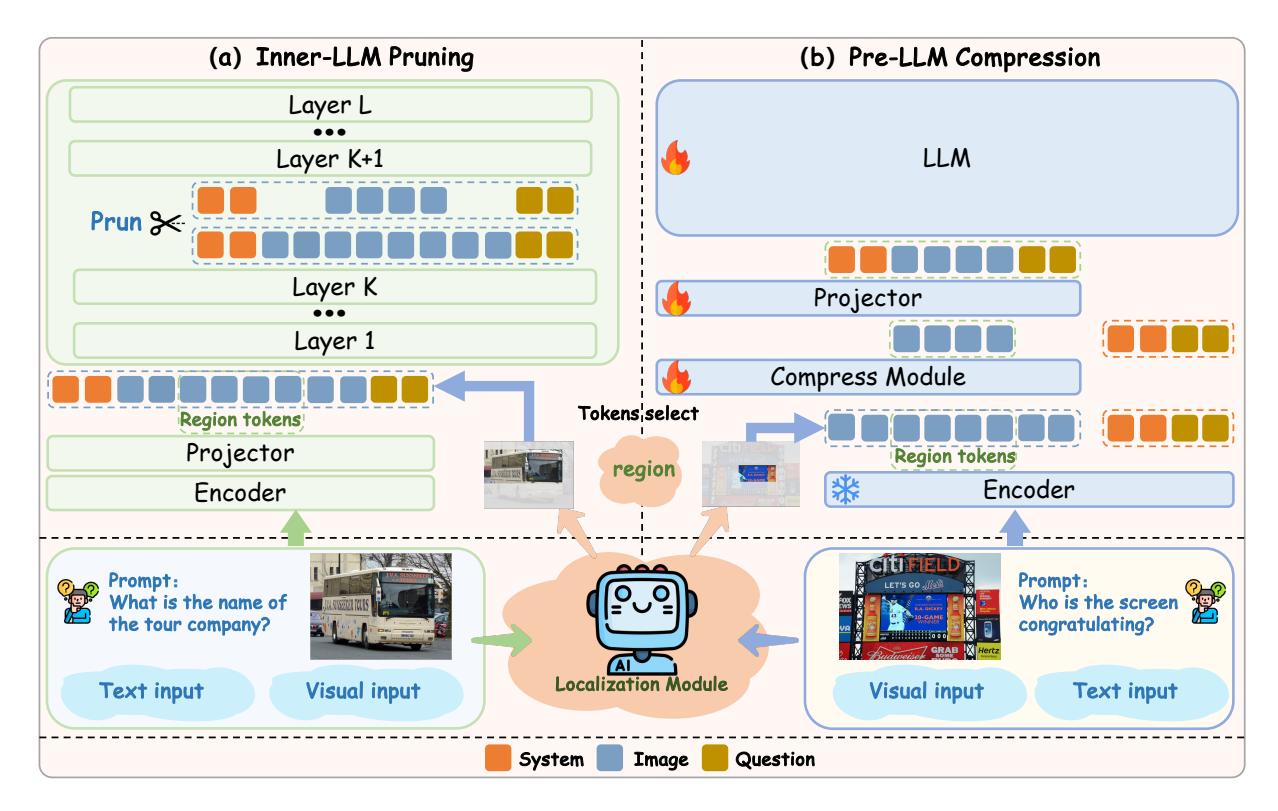


Figure 2: Overview of the CROP framework. Given a visual input and a textual prompt, the Localization Module first identifies task-relevant key regions. This regional information then guides two distinct visual token compression strategies: (a) ILP, where tokens outside the key region are pruned directly within an early layer (Layer K) of the main VLM without retraining it; and (b) PLC, where a dedicated compression module processes tokens from key and non-key regions before they are fed to the LLM. The visual input pipeline and the LLM are shown in context for both strategies.

gions, enabling them not only to answer questions but also to localize relevant areas. For example, Zhang et al. (2025a) highlighted that VLMs might inherently know which visual regions to focus on, even if they occasionally answer questions incorrectly. Shao et al. (2024) showed that cropping and re-inputting relevant image regions can effectively enhance a model's visual perception and introduced datasets for visual region localization. Furthermore, VPT (Yu et al., 2025) incorporated region selection tokens during model training, moving away from precise physical coordinates for grounding tasks. Instead, it describes image regions by dividing the image and using block coordinates, which has been shown to improve localization accuracy.

These studies collectively indicate that VLMs have developed substantial perceptual abilities for question-guided key region localization (Li et al., 2025). Our work builds upon this understanding: by fine-tuning a VLM for explicit region identification, we can generate reliable guidance for our visual token pruning and compression strategies, ensuring that the most salient and contextually complete visual information is preserved.

3 Method

3.1 Overview

To preserve the completeness of key regional information during visual token processing—a factor we hypothesize is crucial for robust understanding compared to methods that might select sparse, disconnected tokens—we introduce Contextual Region-Oriented Vision Token Pruning (CROP). The overall architecture of CROP is illustrated in Figure 2. The framework operates in two main stages: first, a dedicated Localization Module identifies key image regions pertinent to a given query. Second, this regional information guides the subsequent visual token processing in the main VLMs. This approach emphasizes retaining comprehensive visual information within these key regions, particularly their inherent spatial structures and the relationships between constituent patches.

The main VLMs used in our experiments typically process an input image into a grid of visual tokens (e.g., 24×24=576 tokens from ViT-L/14 (Radford et al., 2021)), which maintain spatial correspondence with the original image patches. This spatial mapping is crucial as it allows CROP to

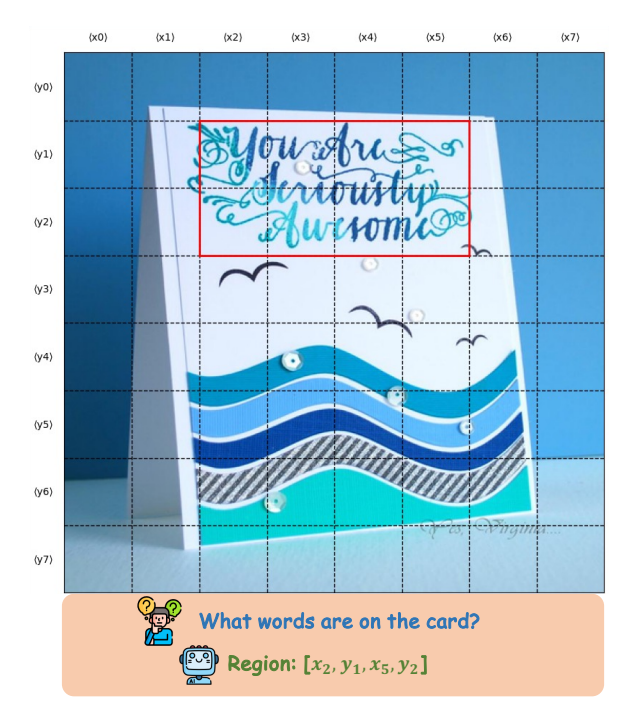


Figure 3: Illustration of the 8×8 Grid-based Region Definition for Key Region Localization. The input image is overlaid with an 8×8 grid. For a given question (e.g., "What words are on the card?"), the Localization Module identifies the key region containing the answer (e.g., the text "You Are Seriously Awesome"). This region is represented by the minimum and maximum 0-indexed block coordinates $[x_{min}, y_{min}, x_{max}, y_{max}]$, which in this example corresponds to $[x_2, y_1, x_5, y_2]$.

accurately translate identified key regions into specific sets of visual tokens for targeted processing. Losing this explicit mapping, as might occur in some global pooling or aggressive token merging strategies, could obscure fine-grained spatial details vital for many VQA tasks. We instantiate and evaluate CROP through two distinct strategies: ILP and PLC. ILP directly removes visual tokens from non-key regions within the early layers of the main VLMs, requiring no retraining. PLC employs a lightweight module to compress visual tokens before they enter the LLM, prioritizing the fidelity of key regional information while integrating broader context.

3.2 Key Region Localization

A lightweight VLM serves as an independent Localization Module, which pre-identifies key regions to provide guidance to the main VLM. Direct bounding box generation by VLMs can be challenging, especially across varied image resolutions. However, guiding models to identify broader regional extents can yield more robust localization. Inspired

by this and approaches like Visual Prompt Tuning (Yu et al., 2025) and Visual-cot (Shao et al., 2024), we developed a specialized training dataset to enhance the Localization Module's ability to discern salient information based on spatial layout. The composition of this dataset is detailed in Table 1.

We represent images on an 8×8 grid, as depicted in Figure 3. A rectangular key region within this grid is defined by block coordinates $[x_{min}, y_{min}, x_{max}, y_{max}]$. These are 0-indexed, meaning each coordinate can range from 0 to 7 inclusive, and must satisfy $0 \le x_{min} \le x_{max} \le 7$ and $0 \le y_{min} \le y_{max} \le 7$.

We selected the Qwen2VL-2B model (Wang et al., 2024) as our Localization Module and finetuned it on this curated dataset. This module, requiring approximately 8 hours of training, achieves high localization accuracy and can be seamlessly integrated as a plug-and-play component with various large VLMs.

3.3 Visual Token Compression

Given the localized key regions, CROP implements ILP and PLC. Our experiments primarily utilize the LLaVA model family (Liu et al., 2023, 2024), which employs a ViT (Dosovitskiy et al., 2021) for visual encoding. In such models, an input image I^v is processed by the visual encoder, and its output features are transformed by a projector (e.g., an MLP) into N^2 visual tokens, $X^v \in \mathbb{R}^{N^2 \times d_h}$. These visual tokens are projected into a space compatible with the text prompt tokens X^T , where d_h is the LLM's hidden embedding dimension. The combined multimodal input for the LLM often follows the structure:

$$\left\langle X_1^q, \dots, X_m^q, X_1^v, \dots, X_{N^2}^v, X_{m+1}^q, \dots, X_{N_t}^q \right\rangle \quad (1)$$

where $\langle X_1^q, \dots, X_m^q \rangle$ is the system prompt, and $\langle X_{m+1}^q, \dots, X_{N_t}^q \rangle$ is the user query.

Inner-LLM Pruning. While some existing methods for reducing visual tokens in VLMs utilize cross-modal attention or introduce additional trainable modules for token selection, our ILP offers a distinct approach. Our observations, consistent with existing literature (Chen et al., 2024, 2023), suggest that VLMs rely more heavily on explicit visual tokens in their earlier layers, with information becoming progressively more abstract and multimodally fused in deeper layers.

ILP leverages this by using the precise, taskrelevant region information from the Localization

Function	Dataset
Region Localization (410k)	TextVQA (73k), Flickr30k (136k), DocVQA (33k) VSR (3k), GQA (88k), OpenImage (43k) CUB (4k), V7W (30k)
Preserving Instruction Following Ability (200k)	Remaining Samples in LLaVA Instruction Tuning (200k)

Table 1: Composition of the training dataset. Our complete training dataset includes the data for training Localization Module in Sec. 4.1 and the remaining portion of the LLaVA-1.5 finetuning dataset. In total, the training dataset comprises 610k samples.

Module. Based on the identified key regions, visual tokens falling outside this area are removed at a designated early layer K of the VLM, as illustrated in Figure 2(a). This approach is truly plug-and-play, as it does not require any retraining of the large VLM. Our experiments validate that this early-stage, region-guided pruning achieves SOTA performance on multiple VQA benchmarks, even for VLMs not specifically adapted for CROP.

Pre-LLM Compression. We hypothesize that key regions contain the most critical visual information for query resolution. To explore this while retaining some global context, PLC is designed as an external, trainable compression module that prioritizes key region fidelity, depicted in Figure 2(b).

Visual tokens from the encoder, X^v , are first partitioned into key region tokens X^{kv} and non-key region tokens X^{nkv} , guided by the Localization Module. We introduce two sets of learnable queries, Q^k and Q^{nk} , to compress these token sets respectively. Positional encodings $P(\cdot)$ are added to queries and tokens before attention. Compression is achieved via scaled dot-product attention (Equations 2 and 3):

$$\hat{X}^{kv} = \operatorname{softmax}\left(\frac{P(Q^k)(P(X^{kv}))^T}{\sqrt{d_h}}\right) P(X^{kv}) \tag{2}$$

$$\hat{X}^{nkv} = \operatorname{softmax}\left(\frac{P(Q^{nk})(P(X^{nkv}))^T}{\sqrt{d_h}}\right) P(X^{nkv})$$
(3)

Here, \hat{X}^{kv} and \hat{X}^{nkv} are the compressed representations.

In addition to the compressed representations, we define anchor tokens X^r to preserve finegrained details. X^r is an 8x8 square patch of 64 tokens, extracted from the original visual encoder output, centered around the geometric midpoint of the key region X^{kv} . These query the compressed key region tokens \hat{X}^{kv} for contextual integration, followed by a residual connection:

$$X^{fused} = \operatorname{softmax}\left(\frac{P(X^r)(P(\hat{X}^{kv}))^T}{\sqrt{d_h}}\right)P(\hat{X}^{kv}) + X^r$$
(4)

The final compressed visual representation \hat{X}^v concatenates the fused key region tokens with the compressed non-key region tokens:

$$\hat{X}^v = \text{Concat}(X^{fused}, \hat{X}^{nkv}) \tag{5}$$

This PLC strategy aims to balance substantial token reduction with the preservation of essential regional details and broader contextual cues.

4 Experiments

4.1 Training Details

All training procedures for CROP were conducted on a server equipped with four NVIDIA GeForce RTX A100 GPUs. The training process is bifurcated into two primary stages:

Stage 1: Localization Module Training The Qwen2VL-2B model was fine-tuned to function as the Localization Module. During this stage, the visual encoder of Qwen2VL-2B was kept frozen, while all other components were trained on our specialized key region localization dataset. The fine-tuning was performed for 2 epochs using the AdamW optimizer with a learning rate of 2e-5. This stage typically completed in approximately 8 hours.

Stage 2: Pre-LLM Compression Module and VLM Co-Fine-tuning For the PLC strategy, the LLaVA-1.5 model was co-fine-tuned with the newly introduced PLC components. Similar to Stage 1, LLaVA's visual encoder remained frozen. The learnable parameters of the PLC module, along with LLaVA's projector and LLM backbone, were jointly optimized. This co-fine-tuning utilized a comprehensive dataset comprising our key region

Method	GQA	MME	$\mathbf{V}\mathbf{Q}\mathbf{A}^{\mathrm{T}}$	$\mathbf{SQA}^{\mathrm{I}}$	\mathbf{VQA}^{V2}	POPE	RelAcc		
<i>Upper Bound, 576 Tokens</i> (100 %)									
LLaVA-1.5-7B	61.9	1862	58.2	69.5	78.5	85.9	100%		
Retain Averaged 192 Tokens (↓ 66.7%)									
FastV	56.5	1786	57.3	69.5	74.6	79.2	95.5% (\ 4.5%)		
SparseVLM	57.6	1721	56.1	69.1	75.6	83.6	95.8% (\ 4.2%)		
PDrop	57.3	1797	56.5	<u>69.2</u>	75.1	82.3	96.2% (\ 3.8%)		
MustDrop	58.2	1787	56.5	<u>69.2</u>	76.0	82.6	96.6% (\ 3.4%)		
VisionZip	59.3	1783	57.3	68.9	76.8	85.3	97.7% (\psi 2.3%)		
VisionZip‡	60.1	1834	57.8	68.2	<u>77.4</u>	84.9	$98.4\% (\downarrow 1.6\%)$		
CROP-ILP	61.3	<u>1817</u>	<u>57.4</u>	<u>69.2</u>	77.7	85.3	98.9% (↓ 1.1%)		
		Retain A	Averaged 1	28 Token	$s (\downarrow 77.8\%$	%)			
FastV	53.0	1646	56.0	69.5	69.2	73.2	90.6% (\$\psi 9.4\%)		
SparseVLM	56.0	1696	54.9	67.1	73.8	80.5	93.4% (\(\psi \) 6.6%)		
PDrop	57.1	1761	56.6	68.4	72.9	82.3	95.2% (\ 4.8%)		
MustDrop	56.9	1745	56.3	68.5	74.6	78.7	94.6% (\ 5.4%)		
VisionZip	57.6	1762	56.8	<u>68.9</u>	75.6	83.2	96.3% (\ 3.7%)		
VisionZip‡	58.9	1823	57.0	68.3	<u>76.6</u>	83.7	$97.4\%(\downarrow 2.6\%)$		
CROP-ILP	60.8	<u>1771</u>	<u>56.9</u>	69.5	76.8	84.4	97.9% (↓ 2.1%)		
		Retain .	Averaged (64 Tokens	(↓88.9%	(b)			
FastV	44.1	1218	50.7	70.0	52.0	55.6	75.9% (\ 24.1%)		
SparseVLM	52.7	1505	51.8	62.2	68.2	75.1	86.5% (\ 13.5%)		
PDrop	47.5	1561	50.6	69.0	69.2	55.9	83.3% (\ 16.7%)		
FasterVLM	51.5	1573	53.1	69.6	66.8	67.2	87.1% (\ 12.9%)		
MustDrop	53.1	1612	54.2	63.4	69.3	68.0	87.4% (\ 12.6%)		
VisionZip	55.1	<u>1690</u>	<u>55.5</u>	69.0	72.4	77.0	92.7% (\psi 7.3%)		
VisionZip‡	57.0	1756	56.0	68.8	74.2	80.9	95.1% (\(\psi 4.9\%)		
CROP-ILP	<u>59.6</u>	1675	54.9	<u>71.5</u>	<u>74.8</u>	83.6	96.0% (\(\psi 4.0\%)		
CROP-PLC	60.3	1634	55.2	71.8	75.0	80.2	$95.4\% (\downarrow 4.6\%)$		

Table 2: **Performance of CROP on LLaVA-1.5-7B compared to existing methods** under three different pruning ratios. The **bold numbers** indicate the best performance achieved by each MLLM, and the <u>underline numbers</u> are the second best.

localization data augmented with standard VQA datasets. Training was conducted for 2 epochs with the AdamW optimizer and a learning rate of 1e-5, requiring approximately 26 hours.

4.2 Experimental Setup

We evaluated our CROP method on LLaVA-1.5-7B and LLaVA-1.5-13B, conducting extensive ablation studies to verify the importance of continuous region preservation for model perception. Experiments were performed across multiple benchmarks (see Appendix for dataset and metric details), with all evaluations adhering to official dataset guidelines and LLaVA's metrics.

For the ILP strategy, pruning was implemented at layer K=2 of the target VLM. Based on the critical regions identified by our Localization Module, visual token pruning rates were set to 66.7%, 77.8%, and 88.9%. A crucial aspect of this setup is that the retained tokens consistently form continuous rectangular image regions. For the PLC strategy, the number of learnable queries for key regions N_{Q^k} and non-key regions $N_{Q^{nk}}$ were con-

figured to 64 and 4, respectively. The number of anchor-preserved tokens N_r from the key region was set to 64.

4.3 Main Results

The primary performance metrics of CROP are presented in Table 2 (for LLaVA-1.5-7B) and Table 3 (for LLaVA-1.5-13B). Across the tested pruning ratios, CROP consistently maintained robust visual comprehension capabilities, achieving SOTA results on several benchmarks.

With the ILP strategy, at a 66.7% visual token pruning rate, LLaVA-1.5-7B and LLaVA-1.5-13B retained 98.9% and 99.7% of their respective baseline performances. Even under a more aggressive 88.9% pruning rate, these models maintained 96.2% (7B) and 95.3% (13B) of their original efficacy. Notably, these ILP results were achieved without any fine-tuning of the LLaVA models.

Our PLC strategy, evaluated on LLaVA-1.5-7B, demonstrated 95.2% performance retention relative to its baseline at an 88.9% visual token pruning rate. These findings strongly validate the effectiveness

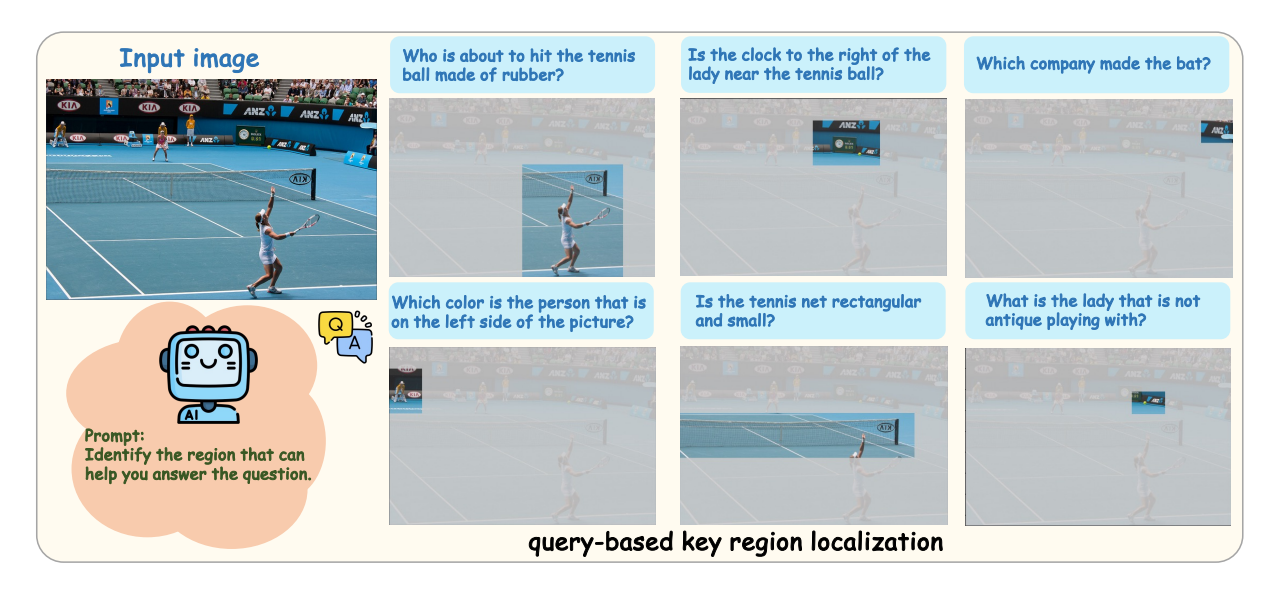


Figure 4: Qualitative examples of query-based key region localization by our Localization Module. For different questions, the module identifies specific, contiguous regions (highlighted) crucial for answering, demonstrating focused attention compared to potentially diffuse attention in other methods.

of CROP, underscoring the benefits of preserving continuous regional information in visual token compression.

Method	GQA	MME	VQA ^T	SQA ^I	VQA ^{V2}	RelAcc		
Upper Bound, 576 Tokens (100%)								
LLaVA-1.5-13B	63.2	1818	61.3	72.8	80.0	100%		
Retain Averaged 192 Tokens (↓ 66.7%)								
FastV	60.3	1807	60.4	74.0	77.7	98.4%		
VisionZip	59.1	1754	59.5	73.5	78.1	97.1%		
VisionZip‡	61.6	1790	59.9	72.7	78.6	98.4%		
CROP-ILP	62.7	1822	60.4	74.2	78.9	99.7%		
Retain	Retain Averaged 128 Tokens (\$\psi\$ 77.8%)							
FastV	57.5	1758	58	73.8	74.3	95.3%		
VisionZip	57.9	1743	58.7	74.0	76.8	96.2%		
VisionZip‡	60.1	1736	59.2	73.0	77.6	96.9%		
CROP-ILP	61.6	1768	59.4	74.1	78.0	98.2%		
Retain Averaged 64 Tokens (↓ 88.9%)								
FastV	50.1	1408	52.2	73.2	61.1	83.8%		
VisionZip	56.2	1676	57.4	74.4	73.7	93.8%		
VisionZip‡	58.1	1671	58.5	72.3	75.2	94.5%		
CROP-ILP	60.4	1708	56.8	73.8	76.0	95.7%		

Table 3: Performance of CROP-ILP with LLaVA-1.5-13B on Various VLM Benchmarks. Results are shown for different pruning ratios compared against the baseline LLaVA-1.5-13B. The **bold values** indicate the best performance.

5 Analyses and Discussion

Previous visual token compression methods have largely overlooked the importance of preserving continuous regions during compression. This section analyzes the impact of our CROP strategy on model perception and understanding, and further evaluates the effectiveness of our Localization Module.

Method	GQA	MME	VQA ^T	SQA ^I	POPE	RelAcc		
Upper Bound, 576 Tokens (100%)								
LLaVA-1.5-7B	61.9	1862	58.2	69.5	85.9	100%		
Retain Averaged 192 Tokens (↓ 66.7%)								
prun	58.7	1735	56.8	69.2	85.4	96.9%		
CROP-ILP	61.3	1817	57.4	69.2	85.3	98.8%		
Retain Averaged 128 Tokens (↓ 77.8%)								
prun	57.9	1734	56.2	69.6	84.6	96.4%		
CROP-ILP	60.8	1771	56.9	69.5	84.4	97.9%		
Retain Averaged 64 Tokens (\pm 88.9\%)								
prun	55.0	1625	54.1	69.9	83.8	93.4%		
CROP-ILP	59.6	1675	54.9	71.5	83.6	96.2%		

Table 4: Performance of LLaVA-1.5-7B with "purn" Guided by the Localization Module. Results are shown across various VQA benchmarks and pruning rates, compared to baseline LLaVA-1.5-7B and representative discrete token pruning methods. The **bold values** indicate the best performance.

5.1 Localization Module's Token Selection

To validate the efficacy of our Localization Module, we conducted experiments on LLaVA-1.5-7B. Using the key regions identified by the module, we derived the corresponding visual token indices. Tokens outside these key regions were pruned entirely before being fed to the LLM, an approach we denote as prun. We tested this at visual token pruning rates of 66.7%, 77.8%, and 88.9%.

As shown in Table 4, even when relying solely on visual information from these localized key regions, the model maintained robust performance.

Method	GQA	MME	$\mathbf{V}\mathbf{Q}\mathbf{A}^{\mathrm{T}}$	SQA ^I	POPE	RelAcc		
Upper Bound, 576 Tokens (100%)								
LLaVA-1.5-7B	61.9	1862	58.2	69.5	85.9	100%		
Retain Averaged 64 Tokens (\psi 88.9\%)								
CROP-PLC	60.3	1634	56.2	71.8	83.7	96.5%		
w/o X^r	56.4	1593	52.3	67.6	81.2	91.7%		

Table 5: Ablation Study on the Impact of Anchor-Preserved Tokens X^r in the PLC Strategy on LLaVA-1.5-7B. Performance is compared between the full CROP-PLC and CROP-PLC(w/o X^r). The results demonstrate that when the anchor tokens X^r are discarded, the model's performance declines as it then processes visual tokens from the key region that are effectively more fragmented. The **bold values** indicate the best performance.

Notably, this simple region-only approach surpassed several meticulously designed discrete token pruning strategies. These results indicate two key findings: (1) our Localization Module accurately identifies critical, query-relevant regions across diverse benchmarks, and (2) retaining tokens from these key continuous regions preserves the majority of essential visual information more effectively than discrete token selection methods.

5.2 Visual Token Selection Strategies

Discrete token pruning strategies, especially those reliant on cross-modal attention, can suffer from attention diffusion. This may lead to the retention of spatially disjointed or peripherally relevant visual tokens that offer limited effective visual guidance. In contrast, CROP's approach, by identifying and preserving continuous regions as illustrated in Figure 4, inherently leverages the contiguity of visual objects and query-specific context. This method focuses the selection on principal visual elements relevant to the query, maintaining spatial coherence and naturally filtering out irrelevant background or edge information. Consequently, CROP yields a more compact and semantically rich set of visual tokens, leading to the improved performance retention validated in our main results.

5.3 Impact of Continuous Region Preservation on Perception

To further quantify the importance of explicitly preserving continuous regional information within our PLC framework, we conducted an ablation study on LLaVA-1.5-7B. We trained a variant of the PLC architecture that omits the anchor-preserved tokens X^{r} and the associated fusion step (Equation 4). In this ablated setup, the visual input to the LLM

comprised only the concatenated compressed representations from key regions \hat{X}^{kv} and non-key regions \hat{X}^{nkv} .

As detailed in Table 5, removing the anchorpreserved tokens X^r led to a notable performance decrease of approximately 5% on average across benchmarks when compared to the full PLC strategy. Furthermore, this ablated PLC variant sometimes underperformed the simpler "prun" strategy (Section 5.1). This finding strongly supports our assertion that explicitly preserving a core set of coherent regional tokens, via mechanisms like the X^r fusion in PLC, is crucial for maintaining the model's perceptual capabilities, especially under aggressive token compression. It suggests that for VLMs, the structural integrity of key visual information can be as important as the individual semantic scores of disparate tokens, a consideration that could inform the design of future token reduction techniques.

6 Conclusion

This work confronts the challenge of computational inefficiency in Vision-Language Models (VLMs) stemming from excessive, often irrelevant, visual tokens—a problem inadequately addressed by prior compression techniques that may disrupt regional coherence or overlook crucial text-image correspondence. We introduced Contextual Region-Oriented Visual Token Pruning (CROP), a framework wherein an efficient Localization Module first identifies query-relevant, contiguous visual regions. This explicit contextual guidance then informs two distinct strategies: the training-free Inner-LLM Pruning (ILP) for direct token removal in early LLM layers, and Pre-LLM Compression (PLC), an adaptive lightweight module. Extensive evaluations demonstrate CROP's substantial improvements over existing methods across multiple VQA benchmarks, with the ILP strategy notably achieving competitive performance without requiring VLM retraining. These findings underscore the critical importance of preserving regional visual integrity for effective token compression, thereby advancing the development of more efficient, robust, and perceptually grounded VLMs and offering a valuable region-oriented paradigm for future multimodal AI research.

7 Limitation

Despite the remarkable efficiency demonstrated by CROP, particularly with its training-free Inner-LLM Pruning (ILP) strategy, the computational gains are primarily observed during inference. The initial fine-tuning of the PLC module, while a one-time cost, does add to the overall model development pipeline. Future work might explore methods to further streamline this initial training phase or develop entirely training-free compression strategies, both internally and externally, such as meta-learning universal compression approaches that require minimal to no task-specific fine-tuning, thereby achieving even more efficient and true "zero-shot" compression.

References

- Jinze Bai, Shuai Bai, Yunfei Chu, Zeyu Cui, Kai Dang, Xiaodong Deng, Yang Fan, Wenbin Ge, Yu Han, Fei Huang, Binyuan Hui, Luo Ji, Mei Li, Junyang Lin, Runji Lin, Dayiheng Liu, Gao Liu, Chengqiang Lu, Keming Lu, and 29 others. 2023. Qwen technical report. *Preprint*, arXiv:2309.16609.
- Liang Chen, Haozhe Zhao, Tianyu Liu, Shuai Bai, Junyang Lin, Chang Zhou, and Baobao Chang. 2024. An image is worth 1/2 tokens after layer 2: Plug-and-play inference acceleration for large vision-language models. *CoRR*, abs/2403.06764.
- Wei-Ge Chen, Irina Spiridonova, Jianwei Yang, Jianfeng Gao, and Chunyuan Li. 2023. Llava-interactive: An all-in-one demo for image chat, segmentation, generation and editing. *Preprint*, arXiv:2311.00571.
- Alexey Dosovitskiy, Lucas Beyer, Alexander Kolesnikov, Dirk Weissenborn, Xiaohua Zhai, Thomas Unterthiner, Mostafa Dehghani, Matthias Minderer, Georg Heigold, Sylvain Gelly, Jakob Uszkoreit, and Neil Houlsby. 2021. An image is worth 16x16 words: Transformers for image recognition at scale. In 9th International Conference on Learning Representations, ICLR 2021, Virtual Event, Austria, May 3-7, 2021. OpenReview.net.
- Chaoyou Fu, Peixian Chen, Yunhang Shen, Yulei Qin, Mengdan Zhang, Xu Lin, Jinrui Yang, Xiawu Zheng, Ke Li, Xing Sun, Yunsheng Wu, and Rongrong Ji. 2024. Mme: A comprehensive evaluation benchmark for multimodal large language models. *Preprint*, arXiv:2306.13394.
- Yash Goyal, Tejas Khot, Douglas Summers-Stay, Dhruv Batra, and Devi Parikh. 2017. Making the v in vqa matter: Elevating the role of image understanding in visual question answering. *Preprint*, arXiv:1612.00837.

- Yuhang Han, Xuyang Liu, Zihan Zhang, Pengxiang Ding, Donglin Wang, Honggang Chen, Qingsen Yan, and Siteng Huang. 2025. Filter, correlate, compress: Training-free token reduction for mllm acceleration. *Preprint*, arXiv:2411.17686.
- Wenxuan Huang, Zijie Zhai, Yunhang Shen, Shaosheng Cao, Fei Zhao, Xiangfeng Xu, Zheyu Ye, and Shaohui Lin. 2024. Dynamic-llava: Efficient multimodal large language models via dynamic vision-language context sparsification. *CoRR*, abs/2412.00876.
- Drew A. Hudson and Christopher D. Manning. 2019. Gqa: A new dataset for real-world visual reasoning and compositional question answering. *Preprint*, arXiv:1902.09506.
- Wentong Li, Yuqian Yuan, Jian Liu, Dongqi Tang, Song Wang, Jie Qin, Jianke Zhu, and Lei Zhang. 2024a. Tokenpacker: Efficient visual projector for multimodal llm. *Preprint*, arXiv:2407.02392.
- Yanwei Li, Yuechen Zhang, Chengyao Wang, Zhisheng Zhong, Yixin Chen, Ruihang Chu, Shaoteng Liu, and Jiaya Jia. 2024b. Mini-gemini: Mining the potential of multi-modality vision language models. *Preprint*, arXiv:2403.18814.
- You Li, Heyu Huang, Chi Chen, Kaiyu Huang, Chao Huang, Zonghao Guo, Zhiyuan Liu, Jinan Xu, Yuhua Li, Ruixuan Li, and Maosong Sun. 2025. Migician: Revealing the magic of free-form multi-image grounding in multimodal large language models. *Preprint*, arXiv:2501.05767.
- Haotian Liu, Chunyuan Li, Yuheng Li, and Yong Jae Lee. 2024. Improved baselines with visual instruction tuning. *Preprint*, arXiv:2310.03744.
- Haotian Liu, Chunyuan Li, Qingyang Wu, and Yong Jae Lee. 2023. Visual instruction tuning. *Preprint*, arXiv:2304.08485.
- Pan Lu, Swaroop Mishra, Tony Xia, Liang Qiu, Kai-Wei Chang, Song-Chun Zhu, Oyvind Tafjord, Peter Clark, and Ashwin Kalyan. 2022. Learn to explain: Multimodal reasoning via thought chains for science question answering. *Preprint*, arXiv:2209.09513.
- Alec Radford, Jong Wook Kim, Chris Hallacy, Aditya Ramesh, Gabriel Goh, Sandhini Agarwal, Girish Sastry, Amanda Askell, Pamela Mishkin, Jack Clark, Gretchen Krueger, and Ilya Sutskever. 2021. Learning transferable visual models from natural language supervision. In *Proceedings of the 38th International Conference on Machine Learning, ICML* 2021, 18-24 July 2021, Virtual Event, volume 139 of Proceedings of Machine Learning Research, pages 8748–8763. PMLR.
- Shuhuai Ren, Linli Yao, Shicheng Li, Xu Sun, and Lu Hou. 2024. Timechat: A time-sensitive multimodal large language model for long video understanding. *Preprint*, arXiv:2312.02051.

- Hao Shao, Shengju Qian, Han Xiao, Guanglu Song, Zhuofan Zong, Letian Wang, Yu Liu, and Hongsheng Li. 2024. Visual cot: Advancing multi-modal language models with a comprehensive dataset and benchmark for chain-of-thought reasoning. *Preprint*, arXiv:2403.16999.
- Zhenwei Shao, Mingyang Wang, Zhou Yu, Wenwen Pan, Yan Yang, Tao Wei, Hongyuan Zhang, Ning Mao, Wei Chen, and Jun Yu. 2025. Growing a twig to accelerate large vision-language models. *Preprint*, arXiv:2503.14075.
- Amanpreet Singh, Vivek Natarajan, Meet Shah, Yu Jiang, Xinlei Chen, Dhruv Batra, Devi Parikh, and Marcus Rohrbach. 2019. Towards VQA models that can read. In *IEEE Conference on Computer Vision and Pattern Recognition, CVPR 2019, Long Beach, CA, USA, June 16-20, 2019*, pages 8317–8326. Computer Vision Foundation / IEEE.
- Peng Wang, Shuai Bai, Sinan Tan, Shijie Wang, Zhihao Fan, Jinze Bai, Keqin Chen, Xuejing Liu, Jialin Wang, Wenbin Ge, Yang Fan, Kai Dang, Mengfei Du, Xuancheng Ren, Rui Men, Dayiheng Liu, Chang Zhou, Jingren Zhou, and Junyang Lin. 2024. Qwen2-vl: Enhancing vision-language model's perception of the world at any resolution. *Preprint*, arXiv:2409.12191.
- Dawei Yan, Pengcheng Li, Yang Li, Hao Chen, Qingguo Chen, Weihua Luo, Wei Dong, Qingsen Yan, Haokui Zhang, and Chunhua Shen. 2024. Tg-llava: Text guided llava via learnable latent embeddings. *Preprint*, arXiv:2409.09564.
- Senqiao Yang, Yukang Chen, Zhuotao Tian, Chengyao Wang, Jingyao Li, Bei Yu, and Jiaya Jia. 2024. Visionzip: Longer is better but not necessary in vision language models. *Preprint*, arXiv:2412.04467.
- Linli Yao, Lei Li, Shuhuai Ren, Lean Wang, Yuanxin Liu, Xu Sun, and Lu Hou. 2024. Deco: Decoupling token compression from semantic abstraction in multimodal large language models. *Preprint*, arXiv:2405.20985.
- Xubing Ye, Yukang Gan, Xiaoke Huang, Yixiao Ge, and Yansong Tang. 2025. Voco-llama: Towards vision compression with large language models. *Preprint*, arXiv:2406.12275.
- Shukang Yin, Chaoyou Fu, Sirui Zhao, Ke Li, Xing Sun, Tong Xu, and Enhong Chen. 2023. A survey on multimodal large language models. *ArXiv preprint*, abs/2306.13549.
- Runpeng Yu, Xinyin Ma, and Xinchao Wang. 2025. Introducing visual perception token into multimodal large language model. *Preprint*, arXiv:2502.17425.
- Xiang Yue, Yuansheng Ni, Kai Zhang, Tianyu Zheng, Ruoqi Liu, Ge Zhang, Samuel Stevens, Dongfu Jiang, Weiming Ren, Yuxuan Sun, Cong Wei, Botao Yu, Ruibin Yuan, Renliang Sun, Ming Yin, Boyuan Zheng, Zhenzhu Yang, Yibo Liu, Wenhao Huang, and

- 3 others. 2024. Mmmu: A massive multi-discipline multimodal understanding and reasoning benchmark for expert agi. *Preprint*, arXiv:2311.16502.
- Jiarui Zhang, Mahyar Khayatkhoei, Prateek Chhikara, and Filip Ilievski. 2025a. Mllms know where to look: Training-free perception of small visual details with multimodal llms. *Preprint*, arXiv:2502.17422.
- Shaolei Zhang, Qingkai Fang, Zhe Yang, and Yang Feng. 2025b. Llava-mini: Efficient image and video large multimodal models with one vision token. *CoRR*, abs/2501.03895.
- Yuan Zhang, Chun-Kai Fan, Junpeng Ma, Wenzhao Zheng, Tao Huang, Kuan Cheng, Denis A. Gudovskiy, Tomoyuki Okuno, Yohei Nakata, Kurt Keutzer, and Shanghang Zhang. 2024. Sparsevlm: Visual token sparsification for efficient visionlanguage model inference. *CoRR*, abs/2410.04417.
- Junjie Zhou, Yan Shu, Bo Zhao, Boya Wu, Zhengyang Liang, Shitao Xiao, Minghao Qin, Xi Yang, Yongping Xiong, Bo Zhang, Tiejun Huang, and Zheng Liu. 2025. Mlvu: Benchmarking multi-task long video understanding. *Preprint*, arXiv:2406.04264.

Appendix

A Template of the Training Data Examples

We now describe our training data format. Both the Localization Module and the PLC strategy's compression module are trained using examples where key regions are defined by the 8x8 grid-based block coordinates presented in Section 3.2. Table 1 provides further details on the datasets used.

Template of Training Example for Region Selection Token

User: <image> <question> Please identify the region that can help you answer the question better.

Assistant: <Region_Selection_Start> <x_min> <y_min> <x_max> <y_max> <Region_Selection_End>.

B Details of Evaluation Benchmarks

In this section, we provide a brief overview of the benchmarks used in our experiments.

GQA (Hudson and Manning, 2019) serves as a benchmark for evaluating visual scene understanding and reasoning capabilities. It utilizes a combination of images, associated questions, and scene graphs, specifically testing a model's ability to grasp spatial relationships and object properties within intricate visual contexts.

MME (Fu et al., 2024) offers a comprehensive assessment of model performance across 14 distinct subtasks, which investigate both perceptual abilities and cognitive skills. The benchmark employs meticulously designed instruction-answer pairs to ensure an equitable and thorough evaluation of a model's multimodal competence. The final reported score represents the aggregate of the perception and cognition scores.

TextVQA (Singh et al., 2019) is designed to gauge a model's capacity to interpret and reason about textual elements found within images. By demanding the synthesis of visual and textual data, it stands as an important benchmark for assessing text-oriented reasoning in visual environments. For conciseness in our experimental tables, we refer to it as "VOA^T".

ScienceQA (Lu et al., 2022) encompasses a broad range of scientific disciplines, including natural, language, and social sciences. Its questions are structured into 26 topics, 127 categories, and 379

skills. This benchmark evaluates a model's multimodal comprehension, aptitude for multi-step reasoning, and its interpretability, thus offering a robust framework for assessing the application of scientific knowledge in visual contexts. In our experiments, we focus exclusively on the image-based samples, denoted as "SQA" in the experimental tables.

VQA-v2 (Goyal et al., 2017) is a comprehensive benchmark consisting of 265,000 images that capture real-world scenes and objects. Each image is presented with open-ended questions, and for each question, ten ground truth answers provided by humans are available.

POPE (Yue et al., 2024) is focused on evaluating object hallucination by presenting binary questions concerning the existence of objects in images. It utilizes metrics such as Accuracy, Recall, Precision, and F1 score, applied over three different sampling methodologies. The score reported reflects the mean accuracy across these three methods: adversarial, random, and popular.

C Benchmarks and Metrics for Evaluation

The benchmarks utilized in our study, along with their respective evaluation metrics, adhere to the official guidelines provided by each benchmark and the official evaluation scripts from the LLaVA model. For the VQA datasets, we assessed the zero-shot question-answering performance using a single input image. All results reported in this paper are averaged across multiple experimental runs.

D More Visualized Results